Nonlinear Response of a Clean One-Dimensional Wire

R. de Picciotto, L. N. Pfeiffer, K. W. Baldwin, and K. W. West
Bell Laboratories, Lucent Technologies, Murray Hill, New Jersey 07974, USA
(Received 21 May 2003; published 23 January 2004)

We study nonlinear transport in a clean one-dimensional wire fabricated by cleaved edge overgrowth in molecular beam epitaxy. At low electron densities, and with a large applied bias, we observe a feature in the differential conductance similar to the so-called "0.7 structure," found in quantum point contact devices. Using a simple model we suggest a link between this phenomenon, charge neutrality, and unidirectional dynamics in the wire.

DOI: 10.1103/PhysRevLett.92.036805 PACS numbers: 73.63.Nm, 73.23.Ad, 05.45.–a

One-dimensional (1D) ballistic wires possess unique electrical properties and have been the subject of numerous studies. Conduction in such wires is often discussed in the context of either the Landauer scattering approach or the Luttinger liquid model. The former is expected to be adequate when the electron-electron interactions do not play a major role, while the latter treats these interactions exactly and thus has a wider range of validity. Both models are applicable with a source-drain bias much smaller than the Fermi energy in the wire. In contrast, the properties of ballistic wires very far from equilibrium, in the presence of a bias comparable to the Fermi energy, are beyond the scope of both models. Here, we examine transport in ultraclean quantum wires in this unusual transport regime.

The hallmark of ballistic electron transport in a 1D wire is the quantization of its linear conductance. In a multimode wire, the overall conductance is given by the conductance quantum, $g_0 = 2e^2/h$, multiplied by the number of available 1D modes. Here e is the charge of an electron and h is Planck's constant. Such ballistic wires have been implemented in a multitude of material systems to date; including split-gate semiconductor quantum point contacts (QPC) [1,2] and wires [3], carbon nanotubes [4], and V-grooved [5] or cleaved edge overgrowth AlGaAs heterostructures [6].

With semiconductor-based wires, a voltage applied to a nearby gate readily controls the 1D charge density, and hence the number of occupied modes can be varied. A resultant conductance-gate voltage trace exhibits a series of quantized conductance plateaus. This quantization of the linear conductance in ballistic wires is a robust phenomenon—insensitive to the system details. All that is required is the absence of backward scattering inside the wire and adiabatic feeding of charge from the reservoirs into the wire.

However, with a large source-drain bias, the differential conductance may deviate from these integer conductance values. For example, in QPC devices, half-integer plateaus were predicted [7] and, indeed, found [8] in the presence of a large bias. More recently, a surprising additional conductance step was noticed in the QPC data [9–18]. At low 1D densities and intermediate biases, the conductance dwells at a value of $\sim 0.7 g_0$ for a finite range of gate voltages.

This so-called "0.7 structure" is a weak feature, distinct from the two main plateau sequences. In QPC devices, it is observed either at intermediate source-drain voltages or, counterintuitively, at somewhat elevated temperatures. The evolution of this structure with bias, magnetic field, and temperature has led to a suggested link between this phenomenon, the spin degree of freedom [9,10], and the Kondo effect [18,19]. Alternatively, an electron-phonon mechanism was recently suggested [20] as a possible origin of this phenomenon.

Here we describe the nonlinear response of a different 1D system. Using the cleaved edge overgrowth (CEO) technique [6], we fabricate long and ultraclean ballistic quantum wires with a length-to-diameter ratio of ~ 100, far larger than in QPC devices. We show that CEO wires share a 0.7-like structure with QPC devices and that at low temperatures this structure occurs whenever the applied bias is as large as 4 times the Fermi energy in the wire.

Linear response studies [21,22] have proven CEO wires to be ultraclean, characterized by a long backscattering length that can exceed 20 μm. The coupling of such CEO wires to their reservoirs, however, falls shy of ideal—leading to a somewhat larger contact resistance and a reduced two-terminal conductance per channel [see inset of Fig. 1(a) and Refs. [6,21,22] for details]. The wire itself, however, is ballistic and resistance-free, as verified by four probe resistance measurements [23].

Differential conductance traces, measured with different values of an applied source-drain voltage, are shown in Fig. 1(a). At low bias, the linear conductance exhibits weak modulations with gate voltage about its mean value of $\sim 0.85 g_0$. As the bias is increased, the mean differential conductance increases while the oscillatory structure diminishes. Instead, a conductance peculiarity emerges at low densities. Similar to the 0.7 structure data from QPCs, this feature becomes more pronounced at larger applied biases. As can be seen in Fig. 1, the conductance is nonmonotonic in this gate voltage range, with a mean

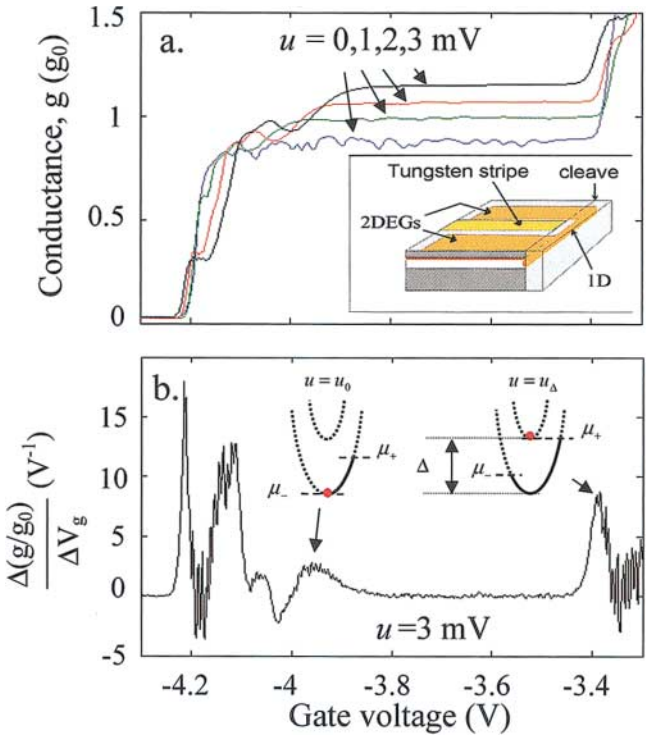

FIG. 1 (color). Differential conductance vs gate voltage at different biases. (a) Differential conductance of a 2 μm long CEO wire at a bath temperature of 18 mK. An ac excitation of 18 μV was used in conjunction with a dc bias of 0, 1, 2, and 3 mV (solid lines). The conductance anomaly at low densities is more pronounced at a larger source-drain bias. Inset: Geometry of a CEO wire: A two-dimensional electron gas (2DEG) is formed in a 25 nm GaAs quantum well by modulation doping. The resultant 2DEG has a carrier density $n_s \approx 2.5 \times 10^{11}$ cm^{-2}, and mobility $\mu \approx 4 \times 10^6$ cm^2/V s. A second modulation doping sequence is then grown onto a freshly cleaved [011] facet to create the 1D wire along the cleaved edge. A tungsten gate evaporated onto the top surface is utilized to deplete the 2DEG and separate out the wire in front of it. The resultant two separate 2DEG sheets are used as source and drain reservoirs. (b) The numerical derivative of the differential conductance at a 3 mV bias [(a), black trace], with respect to the gate voltage. This quantity highlights the transitions between different conductance values, as shown. Inset: the conductance plateau is bound by the second subband at high densities and by depletion of left movers at low densities—see text.

value of about 70% of its plateau [24]. This conductance feature is distinct from yet another conductance step, which occurs at a conductance of $\sim 0.25 g_0$ in our wires [see Fig. 1(a)].

To follow the evolution of the differential conductance with bias and gate voltages, we plot its numerical derivative with respect to the gate voltage—as shown in Fig. 1(b). This quantity measures the sensitivity of the conductance to the charge density *in the wire*. Therefore, the bias dependence of the contact resistance, which is associated with the nongated regions—where the 1D density is fixed, is eliminated from the resultant data. Many such traces, taken at different bias values, allow us to map the conductance changes with both gate voltage and bias—as shown in a color-plot format in Fig. 2. The red lines in the data separate regions of different conductance values, as indicated. Within each region the gate voltage dependence of the differential conductance is weak.

The lowest red line in Fig. 2 separates the zero-conductance state, with a depleted wire, from the finite conductance regions. This pinch-off line exhibits a cusp at small biases. In addition, the aforementioned weak conductance oscillations are visible in the same bias range, at larger gate voltages. Both phenomena disappear at an elevated temperature of 4.2 K (not shown). These features are inconsequential for the present discussion and will be the subject of a separate study.

To analyze these data, we adopt a simple model for transport in a ballistic wire. The relevance of this model stems from the data, as is shown below. Consider free electrons induced by a nearby gate into a clean 1D channel, which is coupled adiabatically to two reservoirs. The chemical potential in the wire is $\mu = \hbar^2 k_F^2/2m$, where m is the effective mass of an electron and the Fermi wave vector, k_F, is related to the electron density, n, and hence to the gate voltage, V_g, via $k_F = (\pi/2)n = (\pi/2)(cV_g/e)$. Here c is the wire-gate capacitance per unit length and the gate voltage is measured with respect to the value

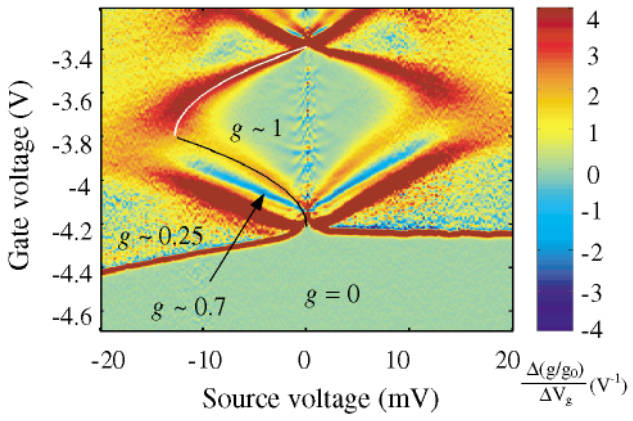

FIG. 2 (color). Transconductance vs gate voltage and dc bias: The numerical derivative of the differential conductance with respect to gate voltage [see Fig. 1(b)] as a function of gate voltage and dc bias, in a color plot format. Data were taken with an ac excitation of 18 μV at a bath temperature of 18 mK. The red lines separate regions of different conductance values, as indicated. The data are largely symmetric with respect to the applied bias. The slight asymmetry results from unintentional device asymmetry that varied from device to device within the 3 wires measured. Superimposed on the data are the curves $u_\Delta(V_g)$, solid white line, and $u_0(V_g)$, solid black line (see text). The onset of the 0.7 anomaly corresponds to the $u_0(V_g)$ curve, which marks the depletion of left (right) movers at a positive (negative) bias.

required to deplete the wire at zero bias. A finite energy gap, Δ, separates the lowest wire mode from the second subband.

To facilitate an electrical current, an imbalance between the electrochemical potentials of the source (right) and drain (left) reservoirs is imposed. This bias, in turn, establishes a difference between the chemical potentials of the left and right propagating electrons in the wire (μ_+ and μ_-, respectively): $\mu_+ - \mu_- = eu$, with u the applied bias. Importantly, the charge density in the wire is nearly independent of this bias—remaining almost equal to the equilibrium one. This arises because with a small gate-wire capacitance, a large potential energy penalty is associated with charge imbalance. Charge neutrality is thus facilitated by a uniform shift of the potential in the wire, such that $\sqrt{\mu_+} + \sqrt{\mu_-} = 2\sqrt{\mu}$. This potential shift reflects the *screening* of the applied bias by the free charges and is accomplished by two potential steps at the inlet and at the outlet of the wire. Note that this potential shift equals half the applied voltage [23] only at voltages much smaller than the Fermi energy.

At low biases, the considerations above are sufficient to calculate the two chemical potentials: $\mu_\pm = \mu(1 \pm eu/4\mu)^2$. Thus, as the bias is increased two unique situations may occur: (a) For $\mu \geq \frac{1}{4}\Delta$, a bias $u_\Delta = 4\mu/e(\sqrt{\Delta/\mu} - 1)$ enforces $\mu_+ = \Delta$. Thus, a bias $u > u_\Delta$ allows the second subband to participate in transport and an increased conductance is expected [see Fig. 1(b)]. (b) Alternatively, for $\mu \leq \frac{1}{4}\Delta$, a bias as large as $u_0 = 4\mu/e$ imposes $\mu_- = 0$. With such a bias, the electrons in the wire are unidirectional and the entire population propagates in the same direction—accounting for the current [see Fig. 1(b)].

Indeed, we find that the line marking an increase in the differential conductance beyond its plateau value corresponds well to the curve $u_\Delta(V_g)$—as shown by the solid white line in Fig. 2. The only free parameter here is the specific capacitance, which we determine to be $c = 18.5 \pm 0.5$ aF/μm. This measured value agrees very well with independent measurements via tunneling spectroscopy in very similar structures [25], as well as with estimates based on the known geometry [26].

Remarkably, we find that at lower densities the curve $u_0(V_g)$, i.e., the bias required for unidirectional dynamics, agrees very well with the onset of the conductance reduction from its plateau value towards the 0.7 structure—as shown in the same figure. Thus, the depletion of left (or right) movers marks the occurrence of this structure. We emphasize that this curve is simply plotted onto the data in Fig. 2 with no additional fitting parameters. The emergence of this boundary points directly to the importance of screening—central to the simple model above.

In Fig. 3(a) we show similar data, taken at larger gate voltages, where the second through sixth wire modes are occupied. As evident from this figure, these data can be fitted to the same model above, again with a striking level

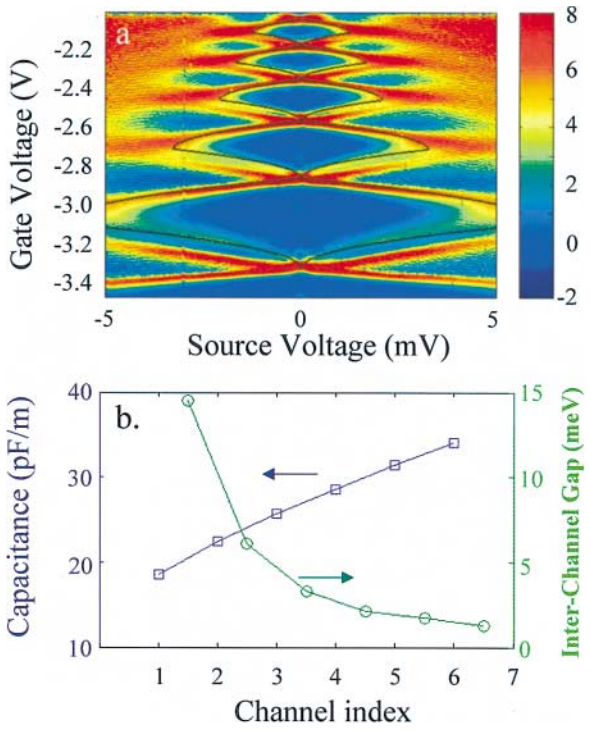

FIG. 3 (color). Transconductance of the upper wire modes: (a) The numerical derivative of the differential conductance with respect to gate voltage, as a function of gate voltage and dc bias in a color plot format. Data were taken with an ac excitation of 18 μV at a bath temperature of 18 mK. The gate voltage range shown corresponds to the second through sixth wire modes. Solid lines: $u_\Delta(V_g)$ and $u_0(V_g)$ curves for each one of the wire modes (see text). (b) Left panel, blue squares: The capacitance between the gate and the ith wire mode, as calculated in a simple model (see text), plotted against the mode index. These capacitance values lead to the excellent agreement with the data in (a) as well as in Fig. 2. Right panel, green circles: the interchannel gaps $\Delta_{i\to i+1}$, as deduced from the data. The confinement energy of the first mode is $\sim$15 meV.

of agreement. However, we find from our fits that the capacitance between the gate to each channel increases by $\sim$10% per channel. As the higher modes of the wire are populated, the capacitance from the gate to each of these modes is, indeed, expected to vary because the transverse charge distribution in the wire is controlled by the mode wave functions and thus varies with the mode index. This "wire diameter" variation is expected to affect the geometrical part of the capacitance logarithmically. In addition, all the wire modes are coupled, both via a direct capacitive coupling and also because all modes share common reservoirs, dictating a common electrochemical potential.

Drawing an analogy to the capacitance of a coaxial cable, we estimate the capacitance between the gate and the ith channel in our CEO wires as $C_i = \alpha 2\pi\varepsilon_0\varepsilon_r / \ln(d/\delta_i)$, where δ_i is the half-width of the wave function of the ith mode, d is the distance to the gate, and a is a

proportionality factor—accounting for the fact that the gate is planar rather than concentric with the wire. Approximating the half-width of the ith mode by $\delta_i = i(100\ \text{Å})$ [23] and using the known wire-gate distance, $d \cong 5000$ Å, we obtain an excellent fit for all the data in both Figs. 2 and 3(a) with a single fitting parameter, $\alpha = 0.1$. This agreement shows that the overall capacitance is dominated by geometry and the corrections due to the density of states or the intermode coupling are negligible, as expected.

This work matches the onset of the 0.7 structure with depletion of either left or right movers in the wire. The conductance value itself ($g \sim 0.7g_0$) remains unexplained, and the existence of yet another flat conductance region ($g \sim 0.25g_0$) is not clarified. A model for a QPC [7] assumes a large number, j, of quasi-1D modes present, and thus ignores screening to predict $g = (j - 1/2)g_0$ at a bias large enough to establish unidirectional dynamics in the jth mode. Thus, with a single mode wire and screening ignored, a conductance of $\frac{1}{2}g_0$ is expected. In contrast, a strictly charge-neutral wire is expected to exhibit a zero differential conductance in this bias range. Once the left movers are depleted, the number of right movers is dictated by charge neutrality; since the resultant current, $I_{\max} = 8(e/h)\mu$, is independent of bias, the differential conductance is expected to vanish. With a finite wire-gate capacitance, a self-consistent solution is likely to yield an intermediate differential conductance; $0 < g < \frac{1}{2}g_0$ and may explain the $g \sim 0.25g_0$ plateau observed here. We emphasize, however, that this plateau occurs at a lower density (or a larger bias) than expected, while a $g \sim 0.7g_0$ feature, not captured by such considerations, persists over an intermediate parameters regime.

Finally, it is worth mentioning that the unique situation of unidirectional electron occupation discussed here is unlikely to occur in linear response at elevated temperatures, where the 0.7 structure is also observed [24]. Thus, the relation between the large-bias–low-temperatures 0.7 structure discussed here and the one observed at high temperatures in linear response clearly represents a further challenge to the theory.

To summarize, we have measured the nonlinear two-terminal conductance of clean and long CEO wires and found a 0.7-like structure. Emphasizing charge neutrality, we suggest a possible link between this phenomenon and the screening properties of a quantum wire in which all electrons are unidirectional.

R. d. P. thanks A. Andreev, B. I. Halperin, K. Matveev, S. H. Simon, H. L. Stormer, A. Yacoby, C. M. Varma, and N. Zhitenev for stimulating discussions.

[1] B. J. van Wees *et al.*, Phys. Rev. Lett. **60**, 848 (1988).
[2] D. A. Wharam *et al.*, J. Phys. C **21**, L209 (1988).
[3] S. Tarucha, T. Honda, and T. Saku, Solid State Commun. **94**, 413 (1995).
[4] S. J. Tans, A. R. M. Verschueren, and C. Dekker, Nature (London) **393**, 49 (1998).
[5] D. Kaufman *et al.*, Phys. Rev. B **59**, R10 433 (1999).
[6] L. Pfeiffer *et al.*, Microelectron. J. **28**, 817 (1997).
[7] L. I. Glazman and A.V. Khaetskii, JETP Lett. **48**, 591 (1988).
[8] L. P. Kouwenhoven *et al.*, Phys. Rev. B **39**, 8040 (1989).
[9] K. J. Thomas *et al.*, Phys. Rev. Lett. **77**, 135 (1996).
[10] N. K. Patel *et al.*, Phys. Rev. B **44**, 10 973 (1991).
[11] B. E. Kane *et al.*, Appl. Phys. Lett. **72**, 3506 (1998).
[12] K. J. Thomas *et al.*, Phys. Rev. B **58**, 4846 (1998).
[13] A. Kristensen *et al.*, Physica (Amsterdam) **249–251B**, 180 (1998).
[14] K. S. Pyshkin *et al.*, Phys. Rev. B **62**, 15 842 (2000).
[15] S. Nuttinck *et al.*, Jpn. J. Appl. Phys. **39**, L655 (2000).
[16] A. Kristensen *et al.*, Phys. Rev. B **62**, 10 950 (2000).
[17] D. J. Reilly *et al.*, Phys. Rev. B **63**, 121311 (2001).
[18] S. M. Cronenwett *et al.*, Phys. Rev. Lett. **88**, 226805 (2002).
[19] Y. Meir, K. Hirose, and N. S. Wingreen, Phys. Rev. Lett. **89**, 196802 (2002).
[20] Georg Seelig and K. A. Matveev, cond-mat/0211579.
[21] A. Yacoby *et al.*, Phys. Rev. Lett. **77**, 4612 (1996).
[22] R. de Picciotto *et al.*, Phys. Rev. Lett. **85**, 1730 (2000).
[23] R. de Picciotto *et al.*, Nature (London) **411**, 51 (2001).
[24] This nonmonotonic behavior diminishes at elevated temperatures. Above $T \sim 2$ K we observe the more common 0.7 conductance step (data not shown).
[25] M. Auslaender *et al.*, Science **295**, 825 (2002).
[26] The wire-gate distance is 0.5 μm, and the wire diameter is ~20 nm [23]. An additional separate gate was evaporated onto the overgrown facet, some 0.3 μm from the wire, and was kept grounded.